View metadata, citation and similar papers at core.ac.uk
brought to you by CORE
provided by RERO DOC Digital Library

Shift of fibril-forming ability of the designed α-helical coiled-coil peptides into the physiological pH region

T.N.Melnik[1], V.Villard[2], V.Vasiliev[1], G.Corradin[2], A.V.Kajava[3] and S.A.Potekhin[1,4]

[1]Institute of Protein Research, Russian Academy of Sciences, 142290 Pushchino, Moscow Region, Russia, [2]Institute of Biochemistry, University of Lausanne, Ch. des Boveresses 155, CH-1066 Epalinges, Switzerland and [3]Centre de Recherches de Biochimie Macromoléculaire, CNRS FRE-2593, 1919 Route de Mende, 34293 Montpellier, Cedex 5, France

[4]To whom correspondence should be addressed.
E-mail: spot@vega.protres.ru

Recently, we designed a short α-helical fibril-forming peptide (αFFP) that can form α-helical nanofibrils at acid pH. The non-physiological conditions of the fibril formation hamper biomedical application of αFFP. It was hypothesized that electrostatic repulsion between glutamic acid residues present at positions (g) of the αFFP coiled-coil sequence prevent the fibrillogenesis at neutral pH, while their protonation below pH 5.5 triggers axial growth of the fibril. To test this hypothesis, we synthesized αFFPs where all glutamic acid residues were substituted by glutamines or serines. The electron microscopy study confirmed that the modified αFFPs form nanofibrils in a wider range of pH (2.5–11). Circular dichroism spectroscopy, sedimentation, diffusion and differential scanning calorimetry showed that the fibrils are α-helical and have elongated and highly stable cooperative tertiary structures. This work leads to a better understanding of interactions that control the fibrillogenesis of the αFFPs and opens opportunities for their biomedical application.

Keywords: design/fibrils/peptides/physico-chemical characteristics

Introduction

The α-helical coiled-coil structures are recognized as one of nature's favorite ways of creating an oligomerization motif. Amino acid sequences of the known coiled-coil structures have a characteristic heptad repeat, $(abcdefg)_n$, with apolar residues in positions (a) and (d) and polar residues generally elsewhere. Proteins with the coiled-coil pattern form two-, three-, four- and five-stranded oligomers depending on variations in their sequences (O'Shea *et al*., 1991; Harbury *et al*., 1993, 1994; Malashkevich *et al*., 1996). The rules governing the stoichiometry of coiled-coils are still intensively tested. We focused our research on the five-stranded coiled-coils (Kajava, 1996; Terskikh *et al*., 1997a). The analysis of their structures suggested that (i) widening of the hydrophobic surface of the α-helix containing apolar (a) and (d) residues by addition of apolar residues at positions (e) or (g) as well as (ii) certain interhelical ionic and hydrogen bonds between side chains in the (b), (c), (e), (f) and (g) positions cause the formation of the five-stranded α-helical coiled-coils (Kajava, 1996). The design of coiled-coils with *a priori* predicted properties is a convincing way to prove our understanding of the principles of coiled-coil oligomerization. Recently, we designed a peptide that was predicted to form a five-stranded coiled-coil fibril with α-helices staggered along the axis. The experiments confirmed that the peptides [called α-helical fibril-forming peptides (αFFPs)] spontaneously form α-helical fibrils with a 2.5 nm diameter at acid pH (Potekhin *et al*., 2001). Such a diameter of the fibrils, the α-helical conformation of the peptide and the orientation of α-helices along the fibril axis agree well with the anticipated five-stranded arrangement. A more comprehensive electron microscopy study suggested that, in addition to the five-stranded protofilaments, the fibrils have another predominant state corresponding to the dimer of the protofilaments (Kajava *et al*., 2003). In recent years the field of the molecular design of α-helical fiber structures has grown (reviewed in Yeates and Padilla, 2002), but, to our knowledge, this is the first α-helical peptide able to form soluble nanofibrils of such small diameter. Previous attempts to obtain α-helical coiled-coil peptides with a potential for axial growth led to fibrous structures, which have a large thickness ranging from ~40 to ~70 nm (Pandya *et al*., 2000; Ogihara *et al*., 2001; Ryadnov and Woolfson, 2003).

This result opens new possibilities for the application of αFFP in biotechnology and medicine. In particular, it was demonstrated that an addition of five to eight amino acid residues to the N-terminus of αFFP does not change the ability of the peptide to form coiled-coil fibrils (Potekhin *et al*., 2001). When designing such a peptide, we had in mind the practical goal of creating a valuable scaffold for the construction of multivalent fusion proteins; in particular, the coiled-coil with the highest number of subunits is especially promising for this purpose (Terskikh *et al*., 1997b). The integration of approximately 100 biologically active peptides in a single fibrillar structure would significantly enhance the efficiency of their binding due to the multivalency of the complex formed. However, the fibrils were formed only at acid pH, and this property limited the number of potential medical applications. Therefore, it was interesting to modify the designed coiled-coil peptide so that it could self-assemble into fibrils at physiological pH.

Materials and methods

Peptide synthesis

Peptides were synthesized on a peptide synthesizer (Applied Biosystems 431A) and purified by RP-HPLC (SS 250×1 cm Nucleosil 300-7 C18 column) using a 0–45% CH_3CN gradient in 0.1% TFA/H_2O for 30 min with a flow rate of 3 ml/min. The purity of the peptides was analyzed by RP-HPLC (C18 analytical column) and mass spectrometry. Peptide concentrations were determined by the method of Waddell based on the difference between spectrophotometric absorptions at 215 and 225 nm (Wolf, 1983), as well as by staining with amido black

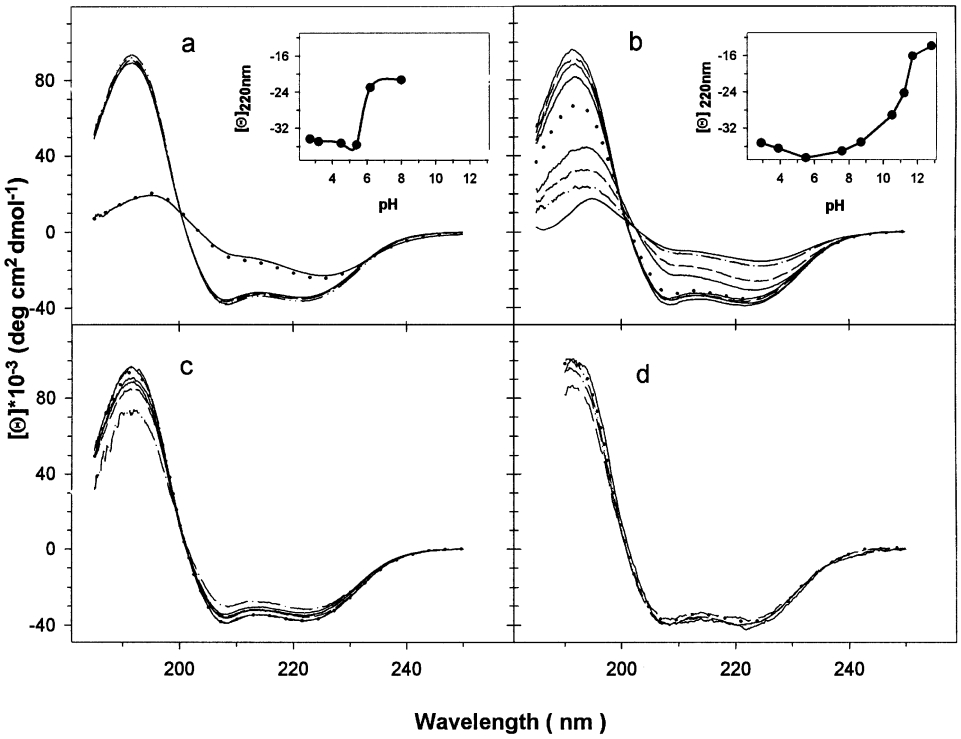

Fig. 1. Far-UV CD spectra of: (**a**) αFFP at pH 2.7 (—), 3.2 (- - -), 4.5 (– · –), 5.4 (–· · –), 6.2 (·····) and 8.0 (—); (**b**) αFFP-2 at pH 2.9 (—), 3.9 (– – –), 5.5 (—), 7.6 (— —), 8.7 (·····), 10.5 (–· · –), 11.2 (- - -), 11.7 (– · –) and 12.8 (– – –); (**c**) αFFP-1 at pH 2.9 (—), 3.1 (– – –), 4.1 (– – –), 6.0 (–· · –), 7.2 (–· · –), 9.3 (·····), 11.0 (- - -) and 12.3 (– · –); (**d**) αFFP-3 at pH 2.9 (—), 6.1 (– – –) and 8.5 (·····). Spectra were recorded at a peptide concentration of 0.1–0.5 mg/ml in 10 mM sodium phosphate buffer at 20°C. Inserts show pH dependence of $[\theta]_{220nm}$ values.

(Schaffner and Weissmann, 1973) and with G-250 (Bradford, 1976).

Circular dichroism (CD) measurements

CD spectra were obtained on a JASCO-600 spectropolarimeter (Japan Spectroscopic Co.) equipped with a temperature-controlled holder in 0.1 mm thick cells at a peptide concentration of 0.1–0.5 mg/ml. The molar ellipticity [θ] was calculated from the equation:

$$[\theta] = \frac{[\theta]_{obs} \cdot M_{res}}{10 \cdot L \cdot C}$$

where $[\theta]_{obs}$ is the ellipticity measured in degrees at the wavelength λ, M_{res} is the mean residue molecular weight of peptide, C is the peptide concentration (g/l) and L is the optical pathlength of the cell (mm). The percentage of α-helicity has been calculated as described in Chen *et al*. (1974).

Sedimentation experiments

Sedimentation experiments were performed in 0.1 M NaCl, 10 mM sodium phosphate, pH 2.8 buffer solutions using a Beckman Model E analytical ultracentrifuge with the Schlieren optical system. The sedimentation coefficient was evaluated at a speed of 42 040 r.p.m. by a standard procedure (Bowen, 1971) at 20°C.

Diffusion experiments

Diffusion coefficients were determined at 20°C from dynamic light scattering experiments using a spectrometer described in detail in Timchenko *et al*. (1990). The laser power was 100–200 μW. Light scattering was measured at an angle of 90°.

An arrival-time correlator was used to extend the range of correlation times. The data were processed using the 'Incorrectness' program developed at the Institute of Protein Research, RAS (Danovich and Serdyuk, 1983). The program allows one to estimate diffusion coefficients for a mixture of particles from the equation for the normalized correlation first-order function $g^{(1)}(t)$:

$$g^{(1)}(t) = \Sigma a_i \ \exp(-D_i q^2 t)$$

where a_i is the portion of scattered radiation of the ith component with the translational diffusion coeffcient D_i, and q is the scattering vector module.

Electron microscopy

The samples were negatively stained with 1% aqueous uranyl acetate using the single-layer carbon technique (Valentine *et al*., 1968). Carbon films of 0.2 nm on freshly cleaved mica were prepared using an electron beam evaporator (Vasiliev and Koteliansky, 1979). Electron micrographs were taken with a JEM-100C electron microscope at an accelerating voltage of 80 kV and magnification of 80 000.

Calorimetric measurements

Calorimetric measurements were made on a precision scanning microcalorimeter SCAL-1 (Scal Co. Ltd, Russia) with 0.33 ml glass cells at a scanning rate of 1 K/min and under a pressure of 2.5 atm (Senin *et al*., 2000). The peptide concentrations ranged from 1.0 to 1.2 mg/ml. The data were analyzed after scan rate normalization and baseline subtraction. The van't Hoff enthalpy was calculated using the usual relationship (Privalov and Potekhin, 1986):

$$\Delta H_{v.H.} = \frac{4 \cdot R \cdot T_m^2}{\Delta H_{cal}} \cdot C_{p,max}$$

where ΔH_{cal} is the calorimetric enthalpy, T_m is the apparent

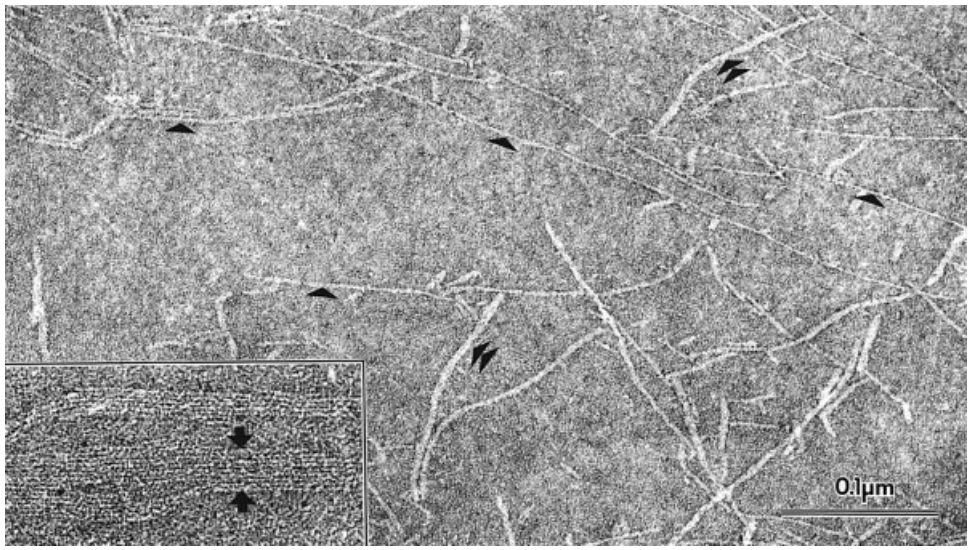

Fig. 2. Electron micrographs of αFFP-2 peptides at pH 2.8 negatively stained by uranyl acetate. Two types of fibrils are seen, their diameters differing approximately two times (marked with single and double arrowheads). The insert shows paracrystalline inclusions observed in the preparations (here αFFP-1 at the same magnification and pH 7.3). The diameter of single-stranded fibrils estimated from the dimensions of such paracrystals is 27 Å.

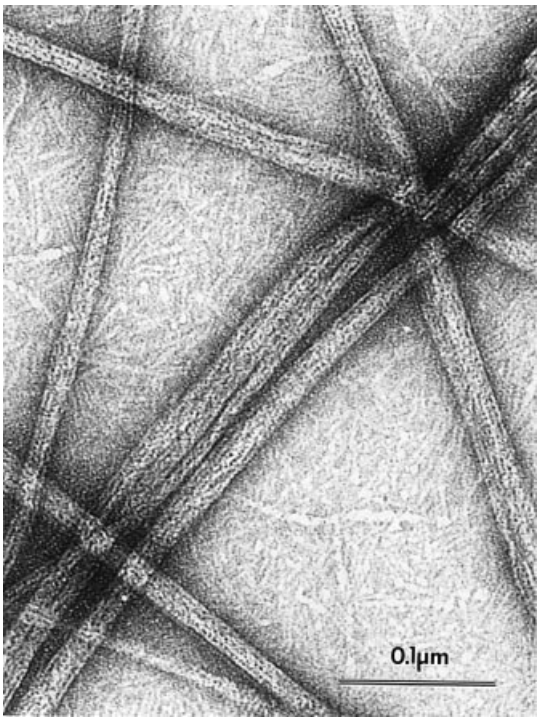

Fig. 3. Electron micrograph of αFFP-3 peptides at pH 7.2 negatively stained by uranyl acetate. In addition to usual strands, uncommonly thick bundles can also be seen.

temperature of denaturation, $C_{p,max}$ is the excess heat capacity at the trace maximum and R is the gas constant.

Results

Peptide design

The original αFFP forms fibrils at acid pH and spherical aggregates at neutral pH (Potekhin *et al*., 2001). The transition between the two states is absolutely reversible, highly cooperative and occurs at pH 5.5–6.0. At this pH, glutamic acid is the most probable group to be deprotonated. However, the shifting of glutamic acid pK_a 4.2–4.4 to 5.5 requires a specific surrounding. Indeed, such a protonation is observed for glutamic acid, which is involved in repulsive electrostatic interactions (Dürr *et al*., 1999; Suzuki *et al*., 1999). Therefore, it was suggested that the electrostatic repulsion between glutamate residues at positions (g) of the αFFP coiled-coil sequence prevents the fibrillogenesis at neutral pH, while their protonation below pH 5.5 triggers the axial growth of the fibril. To enable αFFPs to form fibrils at neutral pH, we substituted all glutamic acid residues by hydrophilic but uncharged glutamines or by serines.

Thus, the following peptides were synthesized: αFFP-1, QLARQL(QQLARQL)$_4$ and αFFP-2, QLARSL(QQLARSL)$_4$. It was also decided to synthesize a peptide αFFP-3, QLAQQL(QQLAQQL)$_4$ where all charged groups, arginine and glutamic acid, are substituted for glutamines.

CD spectroscopy

We used CD spectroscopy to determine the conformation of the synthesized peptides. Figure 1 shows the results of pH titration of the new peptides αFFP-1, -2 and -3 studied at room temperature. In contrast to the original αFFP (Potekhin *et al*., 2001), the new peptides have a high content of α-helical conformation (>95%) not only at acid, but also at neutral pH. The spectra have a maximum at 198 nm and two minima at 208 and 222 nm, characteristic of α-helical conformation. The ellipticity ratio at 220 and 208 nm is ~0.96–1.01, which was suggested to be typical of interacting α-helices (Zhou *et al*., 1994). As seen from the figure, the α-conformation of αFFP-1 (Figure 1c) and αFFP-3 (Figure 1d) is not changed at least up to pH 11.0. The αFFP-2 (Figure 1b) has noticeable conformational changes accompanied by alterations in the CD spectrum when pH is above 9.0. Two specific minima in the spectrum disappear, and at alkaline pH the peptide has a conformation differing from the α-helical one, with slight turbidity of the solution. The insert in Figure 1b shows the titration curve of peptide αFFP-2; it is seen that transition from the α-helical to the non-helical conformation occurs in a wide range of pH (from 9.0 to 12.0) and may reflect the titration of arginine or of the terminal NH_2 group. The peptide does not acquire the

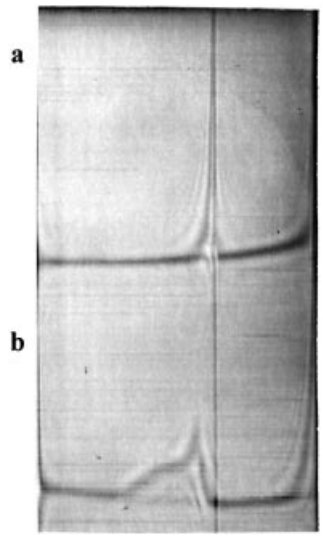

Fig. 4. Sedimentation profiles of peptides αFFP-2 (**a**) and αFFP-1 (**b**) in 10 mM sodium phosphate buffer, 0.1 M NaCl, pH 2.8. The profile was obtained in 32 min after the beginning of centrifugation. Peptide concentration was 0.7 mg/ml.

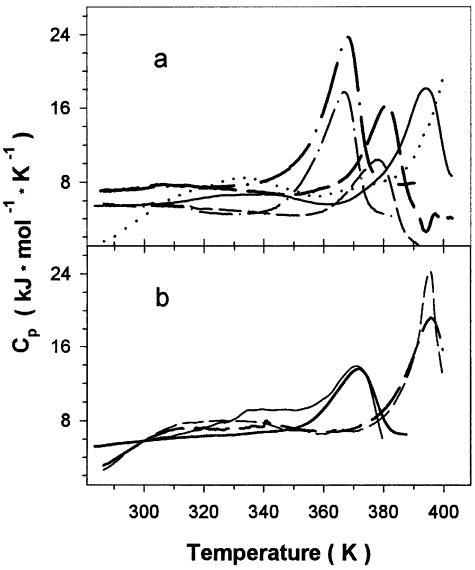

Fig. 5. Temperature dependencies of partial molar heat capacities of αFFP, αFFP-2, αFFP-1 and αFFP-3 in 10 mM sodium phosphate buffer, pH 2.5 at 60% of DMSO (**a**) and in 75% DMSO (**b**). αFFP (—), αFFP-1 (– – –), αFFP-2 (– · –), αFFP-3 (·····). The bold lines correspond to second heatings of peptides. Peptide concentrations were from 0.9 to 1.2 mg/ml.

initial conformation for a period of a few days on return from alkaline to neutral pH. Most likely this is a consequence of the slow kinetics of dissociation of aggregates formed in the alkaline region. It should be noticed that the titration curves for αFFP-2 and αFFP (Potekhin *et al*., 2001) differ greatly in the half-width of transition.

Electron microscopy

The electron microscopy study of the synthesized peptides shows that all of them are able to form fibrils both at acid and neutral pH. Two types of fibrils are observed: thin fibrils of 2.5–3.0 nm in diameter which are apparently five-stranded protofilaments, and twice thicker fibrils (Figure 2). In this case spherical particles seen earlier on the original peptide at neutral pH are not observed at all. Aggregation of αFFP-2 peptides in alkaline conditions leads to the formation of shapeless aggregated material.

Close inspection of the images shows that thick fibrils are formed by association of two protofilaments. This is consistent with our previous electron microscopy study of the original αFFP that revealed single and double protofilaments (Kajava *et al*., 2003). In some cases, the protofilaments are self-oriented in well ordered paracrystalline arrays (inset in Figure 2). Such crystalline formations give an opportunity to measure more accurately the diameter of the protofilament which is 2.7 ± 0.2 nm. The ability of the protofilaments to form paracrystals suggests that they are not flexible, but have an essentially rigid structure.

The observed ratio of single versus double filaments varies significantly. It changes not only from sample to sample but also from field to field of the same sample. Therefore, it does not reflect the real ratio of single and double fibrils in solution. It is possible to assume that double fibrils as well as paracrystals can appear during adsorption of the protofilaments on the surface of a carbon substrate.

It is interesting that a few thicker bundles can be found in the preparations of αFFP-3. Figure 3 shows thick bundles of αFFP-3 formed after binding together of at least five protofilaments.

Table I. Hydrodynamic parameters of fibrils

	$S \times 10^{13}$ (S)	$D \times 10^{7}$ (cm^2/s)	M_w (kDa)[a]	F	f_a/f_b
αFFP	7.03	0.42	1500	6.01	>200
αFFP-1 (E→Q)	5.09	0.32	1400	7.97	>200
αFFP-2 (E→S)	6.42	0.63	920	4.72	150

S is the sedimentation constant in experimental conditions, *D* is the diffusion constant, M_w is molecular weight values evaluated from Svedberg's equation (Bowen, 1971), *F* is Perren's form factor, and f_a/f_b is the axial ratio (Cantor and Schimmel, 1980). The experiments were done in a buffer solution containing 10 mM sodium phosphate buffer, 0.1 M NaCl, pH 2.8 at 20°C. Peptide concentration was 0.7 mg/ml. For αFFP-1 the sedimentation constant of the basic fraction is given.

Hydrodynamics

To assess the dimensions of fibrils in solution, sedimentation and diffusion of the preparations were performed. Figure 4 shows sedimentation profiles for αFFP-2 and αFFP-1 at acid pH. Like the original αFFP, αFFP-2 is represented as a single narrow symmetrical peak at 6.42S, which is close to the sedimentation coefficient of the initial αFFP measured in the same conditions. Although it is evident that the fibril length of the preparation is heterogeneous, this might have no effect on the sedimentation constant and peak diffusion. This is expected since for strongly elongated particles of a constant diameter the sedimentation coefficient depends only a little on their length (Bowen, 1971).

In contrast to the above preparations, heterogeneity of αFFP-1 is well seen on its sedimentation curves. As seen from Figure 4, the preparation contains two fractions with different sedimentation constants. Taking into account that sedimentation constants for both fractions are rather high, it is very likely that the fractions have a fibrillar structure. On the other hand, the sedimentation constant for elongated structures is almost proportional to the square of the section diameter. Thus, it can be postulated that αFFP-1 fibrils, which are present in solution, can have different sections. It is possible that the minor fraction

Table II. Thermodynamic characteristics of peptide denaturation in DMSO solution

		T_m (K)	ΔH_{cal} (kJ/mol)	$\Delta T_{1/2}$ (K)	$\Delta H_{v.H.}$ (kJ/mol)	$\Delta H_{eff}/\Delta H_{cal}$
60% DMSO	αFFP	393.0	179	14.7	360	2.0
	αFFP-1 (E→Q)					
	First run	378.1	121	11.6	417	3.4
	Second run	381.3	121	11.6	417	3.4
	αFFP-2 (E→S)					
	First run	366.8	191	13.2	339	1.8
	Second run	368.2	227	12.0	376	1.7
75% DMSO	αFFP	372.0	125	15.6	295	2.4
	αFFP-3 (E,R→Q)					
	First heat	395.5	[a]	8	650	[a]
	Second heat	395.8		14.6	357	

[a]ΔH_{cal} values could not be calculated because the peptide concentrations defined with various methods differ a few times. T_d (K) is the temperature of the peak maximum, ΔH_{cal} is the calorimetric enthalpy of the basic transition, $\Delta T_{1/2}$ is the half-width of the transition, $\Delta H_{v.H.}$ is the van't Hoff enthalpy. The experiments were performed in a solution containing 10 mM sodium phosphate buffer, 60% DMSO, pH 2.5. The peptide concentrations were 1.0–1.2 mg/ml.

represents two protofilament fibrils detected with electron microscopy.

The results of measuring the sedimentation constants and diffusion coefficients are listed in Table I. The table shows also molecular weights of the preparations calculated by Svedberg's equation. Using the data given in the table, we have calculated Perren form factors (Cantor and Schimmel, 1980) for the studied preparations. They are 6.01, 4.72 and 7.97 for peptides αFFP, αFFP-2 and αFFP-1, respectively. From this analysis it is apparent that all the peptides assemble in rather elongated structures with a large-to-small radius ratio of more than 200 for αFFP and αFFP-1, and 150 for αFFP-2. Thus, αFFP-2 is able to form markedly longer fibrils than the other two. Unfortunately, such measurements for αFFP-3 could not be done owing to a low solubility of the preparation.

Calorimetry

We have found that fibrils formed from αFFP-1, αFFP-2 or αFFP-3 peptides are extremely stable. Similar to the original αFFP, the structures formed by these peptides remain stable in an aqueous solution at least up to 130°C, both at neutral and acid pH. As in our previous paper (Potekhin *et al*., 2001), we used DMSO as a destabilizing agent of peptide structures. Figure 5 shows temperature dependencies of molar heat capacity of the preparations at high DMSO concentrations. Although the fibrils retain an unusually high stability even in DMSO as compared with other proteins (Kovrigin and Potekhin, 1996), they are cooperatively melted at a temperature higher than 365 K. As seen from the figure, the curves have heat absorption peaks that might correspond to cooperative disruption of the structure. That the process is reversible is confirmed by repeated heating of the preparations. It is likely that the preliminary heating of the preparations orders and stabilizes the structure of the fibrils. The main heat absorption peak shifts to higher temperatures (by 2–3 K) (Table II) and the wide minor peak in the pre-denaturation range (290–330 K) decreases or disappears. At the same time, the enthalpy of the basic transition increases.

The structure of αFFP-3 has the highest stability. This structure is stable up to 130°C even in 60% DMSO. Its disruption can be observed only in 75% DMSO at 395.5 K. Thus, its stability exceeds that of the original αFFP by 23.5 K. In contrast to αFFP-3, peptides αFFP-2 and αFFP-1 have a lower stability as compared with that of αFFP. In 60% DMSO the stability of αFFP-1 and αFFP-2 is correspondingly 15 and 26 K lower than that of the original αFFP.

Discussion

The main result of our study is that we succeeded in modifying the *de novo* designed αFFP (Potekhin *et al*., 2001) in such a manner that it can form fibrils not only at acid pH but at neutral pH as well. The fact that the substitution of glutamic acid residues at position (g) of the αFFP coiled-coil sequence shifts the fibril-forming ability of the designed peptides into physiological conditions has clearly demonstrated the correctness of our hypothesis about the factors governing the formation of the fibrils. Another important conclusion is that the fibril-forming ability is not a unique feature of the originally synthesized αFFP peptide (Potekhin *et al*., 2001; Kajava *et al*., 2003) because the modified peptides were able to form morphologically similar fibrils. The exception is αFFP-3; in addition to single and double protofilaments it also has very thick fibrils. The existence of the thick fibrils can be explained by a better complementarity of the hydrogen bond interactions between the protofilaments provided by the glutamine residues of αFFP-3 than by charged residues of the other αFFPs. It is noticeable that the ratio observed for single and double protofilaments varies significantly. This ratio changes not only from sample to sample, but also in different fields of the same sample. Therefore, it is probable that the formation of double protofilaments, at least in some cases, is connected with the preparation of the sample for electron microscopy. On the other hand, a fraction with a larger sedimentation coefficient than that in the main body of the experimental material was found in the αFFP-1 preparation. It cannot be excluded that this fraction represents the double protofilament fibrils that are seen on electron micrographs.

The peptide modification does affect the fibril stability, though not in a crucial way. Both αFFP-1 and αFFP-2 have a highly positive net charge in contrast to neutral αFFP and αFFP-3. The electrostatic repulsion of positive charges can explain the decrease in the stability of αFFP-1 and αFFP-2 fibrils when compared with the original αFFP or αFFP-3. The stability of αFFP-3 fibrils is higher than that of αFFP. This result may be considered as a support of our assumption of the electrostatic repulsion between glutamic acid residues presented at positions (g) of the original αFFP coiled-coil sequence. The substitution of negatively charged glutamic

acid for glutamine may eliminate this repulsion and increase the fibril stability.

The titration curves obtained by CD spectroscopy show that the fibrils formed with peptides αFFP-1 and αFFP-3 have no conformational changes at least up to pH 11. Inasmuch as αFFP-3 has no titrated changed side groups, it may be concluded that titration *per se* of the N-terminal amino group and the C-terminal carboxyl group cannot affect the ability of the peptides to form fibrils. On the other hand, αFFP-1 contains arginines at position (f) that can also undergo titration, but at very high pH. As expected, titration to pH 11 does not affect the formation of fibrils.

Attention should also be paid to one more feature of titration of the initial peptide and αFFP-2. As seen from titration curves of αFFP, fibrils are disrupted at pH ~6.0, probably due to the anomalous titration of glutamic acid residues. The half-width of the transition shows that the process is cooperative. Fibrils of αFFP-2 are disrupted as a result of titration of arginines, the process being non-cooperative.

It was also shown that the substitution of residues at the coiled-coil position (g) of αFFP might favor the formation of well ordered paracrystalline arrays. This is an important result not only for an accurate estimation of the diameter of the protofilaments but also for a further application of these peptides in optics and nanotechnology. Indeed, when oriented such nanofibrils can form materials with an anisotropic transmitting capability.

The ability of a series of αFFPs to form fibrils at physiological conditions also opens new perspectives for their application in biotechnology and medicine. For example, a soluble oligomer with such a large number of subunits is especially promising as a scaffold for the construction of multivalent fusion proteins. In this case, a large number of copies of the biologically active ligands may protrude from the fibril body and impart high multivalency to the complex. This property of αFFP can be widely used in medical treatments and biotechnological processes where a higher efficiency can be achieved by associating a larger number of functional subunits into one complex (Terskikh *et al*., 1997b).

Acknowledgements

We thank D.Prokhorov for the assistance in the diffusion experiments and V.Brossard for the peptide purification. The authors gratefully acknowledge the financial support from the Swiss National Science Foundation (grant no. 7SUPJ062317) and from the Russian Foundation for Basic Research (grant no. 02-04-48737).

References

Bowen,T.J. (1971) *An Introduction to Ultracentrifugation.* Wiley-Interscience, London.

Bradford,M.M. (1976) *Anal. Biochem.*, **72**, 248–254.

Cantor,C.R. and Schimmel,P.R. (1980) *Biophysical Chemistry*. W.H.Freeman, San Francisco, Vol. 2.

Chen,Y.H., Yang,J.T. and Chau,K.H. (1974) *Biochemistry*, **13**, 3350–3359.

Danovich,R.D. and Serdyuk,I.N. (1983) In Shulz-DuBois,E.O. (ed.), *Proton Correlation Techniques in Fluid Mechanics*. Springer, Berlin, pp. 315–321.

Dürr,E., Jelesarov,I. and Bosshard.,H.R. (1999) *Biochemistry*, **38**, 870–880.

Harbury,P.B., Zhang,T., Kim,P.S. and Alber,T. (1993) *Science*, **262**, 1401–1407.

Harbury,P.B., Kim,P.S. and Alber,T. (1994) *Nature*, **371**, 80–83.

Kajava,A.V. (1996) *Proteins*, **24**, 218–226.

Kajava,A.V., Potekhin,S.A., Corradin,G. and Leapman,R.D. (2003) *J. Pept. Sci.*, in press.

Kovrigin,E.L. and Potekhin,S.A. (1996) *Biofizika*, **41**, 1201–1206.

Malashkevich,V.N., Kammerer,R.A., Efimov,V.P., Schulthess,T. and Engel,J. (1996) *Science*, **274**, 761–765.

Ogihara,N.L., Ghirlanda,G., Bryson,J.W., Gingery,M., De-Grado,W.F. and Eisenberg,D. (2001) *Proc. Natl Acad. Sci. USA*, **98**, 1404–1409.

O'Shea,E.K., Klemm,J.D., Kim,P.S. and Alber,T. (1991) *Science*, **254**, 539–544.

Pandya,M.J., Spooner,G.M., Sunde,M., Thorpe,J.R., Rodger,A. and Woolfson,D.N. (2000) *Biochemistry*, **39**, 8728–8734.

Potekhin,S.A., Melnik,T.N., Popov,V., Lanina,N.F, Vazina,A.A., Rigler,P., Verdini,A.S., Corradin,G. and Kajava,A.V. (2001) *Biol. Chem.*, **8**, 1025–1032.

Privalov,P.L. and Potekhin,S.A. (1986) *Methods Enzymol.*, **131**, 1–51.

Ryadnov,M.G. and Woolfson,D.N. (2003) *Nat. Mater.*, **2**, 329–332.

Schaffner,W. and Weissmann,C. (1973) *Anal. Biochem.*, **56**, 502–514.

Senin,A.A., Potekhin,S.A., Tiktopulo,E.I. and Filimonov,V.V. (2000) *J. Therm. Anal. Calorimetry*, **62**, 153–160.

Suzuki,K., Yamada,T. and Tanaka,T. (1999) *Biochemistry*, **38**, 1751–1756.

Terskikh,A.V., Potekhin,S.A., Melnik,T.N. and Kajava,A.V. (1997a) *Lett. Pept. Sci.*, **4**, 297–304.

Terskikh,A.V., Le Doussal,J.M., Crameri,R., Fisch,I., Mach,J.P. and Kajava,A.V. (1997b) *Proc. Natl Acad. Sci. USA*, **94**, 1663–1668.

Timchenko,A.A., Griko,N.B. and Serdyuk,I.N. (1990) *Biopolymers*, **29**, 303–309.

Valentine,R.S., Shapiro,B.M. and Stadtman,E.R. (1968) *Biochemistry*, **7**, 2143–2152.

Vasiliev,V.D. and Koteliansky,V.E. (1979) *Methods Enzymol.*, **59**, 612–629.

Wolf,P. (1983) *Anal. Biochem.*, **129**, 145–155.

Yeates,T.O. and Padilla,J.E. (2002) *Curr. Opin. Struct. Biol.*, **4**, 464–470.

Zhou,N.E., Kay,C.M. and Hodges,R.S. (1994) *J. Mol. Biol.*, **237**, 500–512.

Received July 7, 2003; revised October 27, 2003; accepted October 30, 2003